

Article

# Signal Intensity of Contrast Enhancement according to TE in 3.0T MRI T1 Imaging

Hyun Keun Jeong<sup>1</sup>, Kwon Hee Lee<sup>1</sup>, Min Hee Kim<sup>2</sup>, Sung Ho Kim<sup>1</sup>, Min Gi Kim<sup>1,\*</sup> and Ho Chul Kim<sup>2,\*</sup>

<sup>1</sup> Department of Bio-Medical Science, Korea University, 145 Anam-ro Sungbuk-ku, Seoul 02841, Korea; sinarbro@hanmail.net (H.K.J.); iamken1223@korea.ac.kr (K.H.L.); 20050508@kuh.ac.kr (S.H.K.)

<sup>2</sup> Department of Radiological Science & Physical Medicine, Eulji University, 553 Sanseong-daero Soojung-ku Sungnam-city, Kyunggi-do 13135, Korea; minxi1004@gmail.com

\* Correspondence: mgkim@korea.ac.kr (M.G.K.); tiger1005@eulji.ac.kr or tiger1005@gmail.com (H.C.K.); Tel.: +82-10-8934-6412 (M.G.K.); +82-10-8800-5114 (H.C.K.)

Received: 12 June 2018; Accepted: 11 July 2018; Published: 13 July 2018



**Abstract:** Normal body tissue or lesion characteristics in T1 images have been evaluated; however, how external parameters effect the change in signal intensity by gadolinium-based contrast agent remains unknown. We investigated how contrast enhancement changed according to echo time (TE) in 3.0T magnetic resonance (MR) T1 imaging and determined the optimal settings for TE in contrast-enhanced T1 imaging. Since there are no guidelines regarding parameters for T1 enhancement when using MR-contrast agents, we analyzed results from varying TEs (between 25 and 7 msec) in both a phantom and clinical study. We obtained the following results: contrast percentage of fat to saline increased from 740.0–1003.6%, response start point increased from 30–90 mmol, max peak signal intensity increased from 1771–2425 a.u., max peak point increased from 2–4 mmol, enhancement percentage of the max peak signal intensity (MPSI) to saline increased from 1671.0–2065.2%, the average of SI on each mol as TE increased from 600.8–996.6 a.u., the average of SI as TE on each molar concentration increased from 378–845 a.u., the AEPSS increased from 44.3–140.3%, and the AEPSC increased from 224.3–647.8%. We confirmed that TE can affect contrast enhancement, and the lowest TE has faster and higher effects on contrast enhancement.

**Keywords:** 3.0T MRI; contrast enhancement; gadoteridol; contrast media; echo time; T1 imaging

## 1. Introduction

Magnetic resonance imaging (MRI) is achieved through the paramagnetism of the hydrogen (<sup>1</sup>H) protons in the body when placed in a magnetic field. Thus, <sup>1</sup>H protons in various tissues emit different energy signatures depending on the proton relaxation rate in that tissue. MRI displays these energy differences as contrast in a scan image [1,2]. Generally, the MRI signal intensity (SI) is determined by the gradient strength ( $M_0$ ), flip angle ( $\alpha$ ), repetition time ( $TR$ ), echo time ( $TE$ ),  $1/T_1$  ( $R_1$ ), and  $1/T_2^*$  ( $R_2^*$ ), as shown in Equation (1) [3,4];

$$SI = M_0 \sin(\alpha) \cdot \frac{1 - e^{-R_1 \cdot TR}}{1 - \cos(\alpha) \cdot e^{-R_1 \cdot TR}} \cdot e^{R_2^*(*)TE} \quad (1)$$

Of the factors that determine the SI;  $\alpha$ ,  $TR$ ,  $TE$ , and  $M_0$  are external factors that can be intentionally controlled from the MRI apparatus.  $R_1$  and  $R_2$ , on the other hand, are unique properties of <sup>1</sup>H protons in a given magnetic field, and cannot be controlled externally. However, it is possible to increase the SI, for diagnostic purposes, by adjusting  $R_1$  relaxation and  $R_2$  decay; this is achieved using a gadolinium-based contrast agent (GBCA). GBCAs are administered for MRI to enhance the SI of

lesions and to increase the diagnostic value of the imaging technique. In vivo, gadolinium interacts with the normal  $^1\text{H}$  spins to reduce the  $R_1$  and  $R_2$  relaxation times. These  $^1\text{H}$  protons show faster relaxivity than  $^1\text{H}$  protons that are not bound to gadolinium, producing a high SI in MRI images compared to the usual positive magnetic susceptibility [1,2]. In humans, MRI can be applied to various indications, and in terms of contrast-enhanced imaging using GBCA, contrast-enhanced (CE)-T1 is especially often used in clinical settings. Diagnostically, MRI is useful to evaluate the presence or absence of tumors. Previous studies have only addressed the characteristics of normal body tissues or lesions in T1 images according to sequences and have also shown clinical comparison data according to GBCA concentration. However, how the change in the SI of GBCA is affected by external parameters is currently unknown [5–7]. Here, we can surmise that the parameters controlling MR physics will affect the relaxation of the  $^1\text{H}$  spin that is bonded to gadolinium. This is because the signal strength of each tissue, with different relaxation rates, can be controlled by external parameters. In this study, the main parameters determining the MR SI are TR and TE, as shown in Equation (1). In a conventional spin echo (SE) sequence, TR refers to the time from one  $90^\circ$  RF pulse to the next  $90^\circ$  RF pulse, while TE refers to the time from the RF pulse to the echo. The TR and TE parameters can be used to adjust the image contrast in different tissues with different relaxation times. Clinically, in order to achieve a T1 effect in humans, TR is usually in the range 200–600 msec and TE in the range 10–25 msec [8–10]. It is common to use a  $90^\circ$  excitation angle and a  $180^\circ$  refocusing angle for flip angles (FAs). Since TR is directly related to the acquisition time per slice, it is set as low as possible. Thus, in clinical settings, routine values are used for TR and FA, but in the case of TE, there is no specific guideline for CE-T1 in 3.0T MRI. Therefore, in this study, we quantitatively analyzed the SI change of gadolinium, according to TE regulation, through MR in both phantom and clinical tests, and suggested a proper TE value for T1 enhancement.

## 2. Materials and Methods

This study was conducted according to the clinical criteria of the Eulji University Institutional Review Board (IRB) and, after review, was registered with the administration number EUIRB2018-8 (Title: Contrast enhancement according to TE at 3.0T MRI brain T1 image) approved on 3 January 2018.

### 2.1. Phantom Study

#### 2.1.1. Preparation of GBCA and the MR Phantom

For the MR-contrast agent, we used 500 mmol (0.5 mol) gadoteridol (ProHance; Bracco, Milan, Italy) [11]. The MR phantom (size:  $175 \times 243 \times 8.7$  cm, made from non-magnetic material) was constructed according to the design in Figure 1a,b. The phantom consisted of 30 containers; as shown in Table 1. Containers 1–29 were filled with 0.5 mol gadoteridol diluted to various concentrations in the range 0–500 mmol, and the final container was filled with fat (cooking oil). Through this MR phantom study, used to mimic the administration of the drug to the body, we aimed to quantify the signal change in each container from the TE change corresponding to the degree of gadoteridol dilution.

**Table 1.** GBCA concentration and dilution rate in the phantom study.

No.	Saline (mL)	GBCA (mL)	Gadoteridol (mmol)	Dilution Rate (%)	No.	Saline (mL)	GBCA (mL)	Gadoteridol (mmol)	Dilution Rate (%)
1	0.00	30	500	100	16	29.52	0.48	8	1.60
2	6.00	24	400	80	17	29.58	0.42	7	1.40
3	12.00	18	300	60	18	29.64	0.36	6	1.20
4	18.00	12	200	40	19	29.70	0.3	5	1.00
5	24.00	6	100	20	20	29.76	0.24	4	0.80
6	24.60	5.4	90	18	21	29.82	0.18	3	0.60
7	25.20	4.8	80	16	22	29.88	0.12	2	0.40
8	25.80	4.2	70	14	23	29.94	0.06	1	0.20
9	26.40	3.6	60	12	24	29.95	0.048	0.8	0.16
10	27.00	3	50	10	25	29.96	0.036	0.6	0.12
11	27.60	2.4	40	8	26	29.97	0.024	0.4	0.08
12	28.20	1.8	30	6	27	29.98	0.012	0.2	0.04
13	28.80	1.2	20	4	28	29.99	0.006	0.1	0.02
14	29.40	0.6	10	2	29	30.00	0	0	0.00
15	29.50	0.54	9	1.80	30	fat			

GBCA, gadolinium-based contrast agent; No., number.

### 2.1.2. MRI Specification and Protocol

#### (1) MRI specification

For this study, we used a Siemens Skyra 3.0T model MRI and 20ch head coil, as shown in Figure 1c.

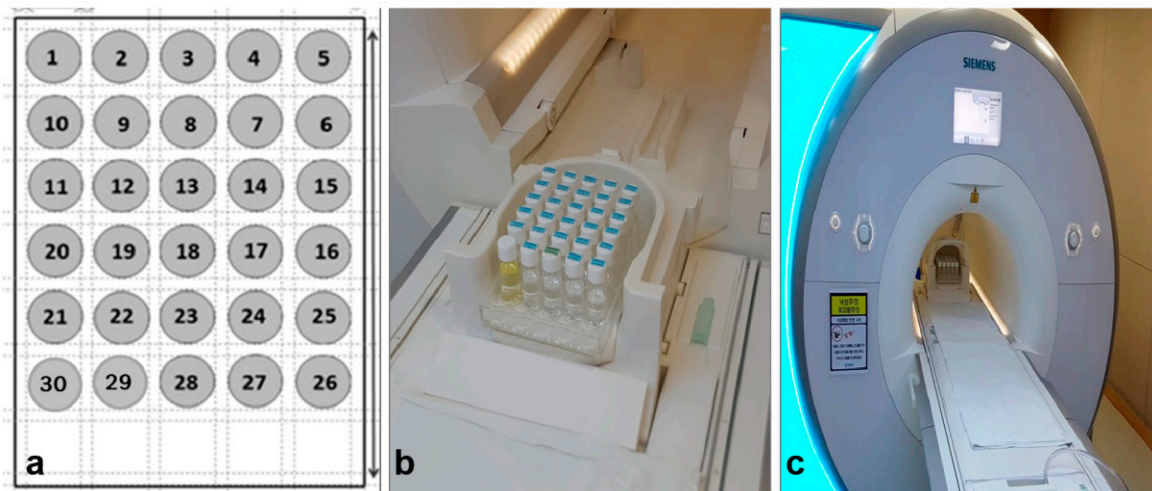


**Figure 1.** MR phantom and MRI apparatus. (a) Schematic diagram of the MRI phantom; (b,c) photographs of the MR phantom and apparatus. MR, magnetic resonance; MRI, magnetic resonance imaging.

#### (2) Sequence and parameters

We used a conventional SE sequence for T1 imaging. First, the MR phantom was loaded into the head coil, as shown in Figure 1b. TE, which was the parameter of interest in this study, decreased from 25 to 7 msec in seven steps, as shown in Table 2. All other parameters were kept constant.

Table 2. MR phantom parameters.

	Unit	1st	2nd	3rd	4th	5th	6th	7th
Sequence		SE						
TE	msec	25	22	19	16	13	10	7
TR	msec	300	300	300	300	300	300	300
FOV	mm	240	240	240	240	240	240	240
Thickness	mm	5	5	5	5	5	5	5
Flip Angle	°	50	50	50	50	50	50	50
Average		1	1	1	1	1	1	1
BW	Hz/Px	130	130	130	130	130	130	130
Acquisition Time		2:11	2:11	2:11	2:11	2:11	2:11	2:11

MR, magnetic resonance; TE, echo time; TR, repetition time; FOV, field of view, BW, bandwidth.

### 2.1.3. Experimental Procedure

The experiment proceeded according to Figure 2. In total, 20 scans were performed identically. The mean SI for each of the 30 phantom containers was measured from the cross-sections, and used to calculate the overall mean SI.

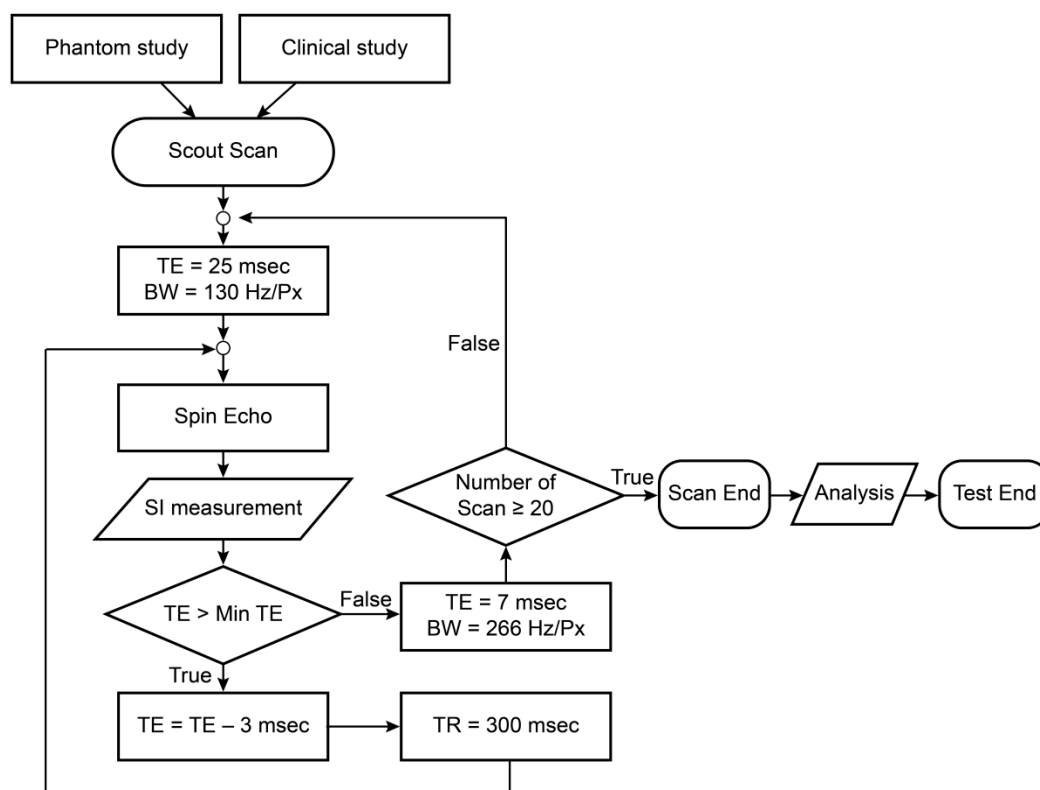
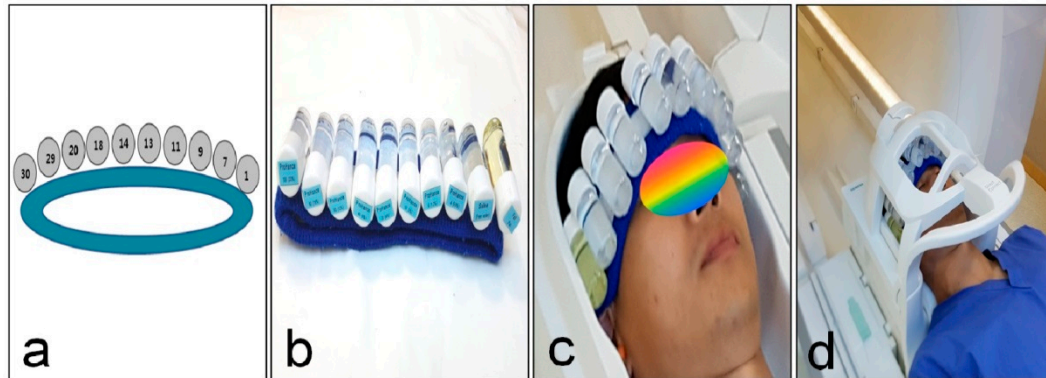


Figure 2. Study flowchart. TE, echo time; BW, bandwidth; TR, response time.

### 2.2. Clinical Study

The clinical study was conducted on one healthy volunteer. For the clinical study, a clinical phantom was constructed according to Figure 3a,b. The purpose of the clinical phantom was to treat each container as a lesion, and to provide a direct comparison of the change in signal by GBCA dilution rate with the SI of the brain tissue. To this end, 10 containers, each containing a different concentration of GBCA, were attached to a non-magnetic headband; the containers used were containers 1, 7, 9, 11, 13, 14, 18, 20, 29, and 30 from Table 1. As shown in Figure 3c,d, the headband was strapped to the

volunteer's head, and the contrast enhancement was compared, by concentration, with the actual brain images. The procedure for the clinical study was the same as with the phantom study. Since individual differences in the white and gray matter of the brain can cause differences in the signal for a given setting, we performed 20 scans on a single volunteer.



**Figure 3.** Images of the clinical study, (a,b) clinical phantom design and photographs; (c,d) the setup of the clinical study.

### 2.3. Method of Analysis

The Medical Standard's PACSPLUS program was used to measure SI in both the phantom and clinical studies. Regions of interest (ROIs), depicted as a green ellipse (Area = 4.5 cm<sup>2</sup>, 650 px) in Figure 3b, were selected in the cross-section of containers with different GBCA concentrations, and the mean SI was measured for each container. In order to quantitatively analyze the degree of enhancement according to the TE change in the phantom study, the following nine evaluation criteria were set: (1) the saline signal intensity of phantom study (SSI<sup>1</sup>), which is similar to free water in the body; (2) the fat signal intensity of the phantom study (FSI<sup>1</sup>); (3) the contrast percentage of fat to saline (CPFS) was calculated as the contrast between SSI<sup>1</sup> and FSI<sup>1</sup>, expressed as a percentage; (4) the response start point (RSP) was the point at which signal enhancement could be observed with the naked eye (SI ≥ 40 a.u.); (5) the max peak signal intensity (MPSI) was the highest SI; (6) the max peak point (MPP) was the point at which the MPSI was detected; (7) the enhancement percentage of MPSI to saline (EPMS) was the signal enhancement of the MPSI relative to free water; (8) the enhancement percentage for each mol (EP mmol) was the signal enhancement for each GBCA concentration; and (9) the average of SI for each mol per TE (AST) was the mean SI across all concentrations at each TE. Here, CPFS, EPMS, and EP were calculated by the following Formulas (2)–(4):

$$\text{CPFS} = ((\text{FSI} - \text{SSI}) / \text{SSI}) \times 100 \quad (2)$$

$$\text{EPMS} = (\text{MPSI} - \text{SSI}) \times 100 \quad (3)$$

$$\text{EP} = ((\text{SI on each mmol} - \text{SI on previous mmol}) / \text{SI on previous mmol}) \times 100 \quad (4)$$

In the clinical study, the following nine quantitative criteria were established to compare the contrast between the extent of enhancement and brain parenchyma according to TE changes: (1) the saline signal intensity of the clinical study (SSI<sup>2</sup>) was the SI of saline in the clinical phantom; (2) the fat signal intensity of clinical study (FSI<sup>2</sup>) was the SI of fat in the 2nd phantom; (3) the SC was the SI of the intraventricular CSF; (4) the SBP was the SI of brain parenchyma; (5) the average SI by TE for each molar concentration (ASTM) was the SI for each TE averaged across all molar concentrations; (6) the enhancement percentage of the SI for each mol by SBP (EPSS of each mol) was calculated as the contrast between the SBP and the GBCA SI at each concentration, expressed as percentages; (7) the AEPSS was the average of EPSS; (8) the enhancement percentage of SI for each mol by SC (EPSC

of each mol) was calculated as the contrast between the SC and the GBCA SI at each concentration, expressed as percentages; and (9) the AEPSC was the average of EPSC. Here, the EPSS and EPSC were calculated by the following formulas (5) and (6):

$$\text{EPSS} = ((\text{SI on each mmol} - \text{SBP})/\text{SBP}) \times 100 \quad (5)$$

$$\text{EPSC} = ((\text{SI on each mol} - \text{SC})/\text{SC}) \times 100 \quad (6)$$

#### 2.4. Statistical Analysis

Each result calculated in the clinical study was analyzed by statistical methods using SPSS for Windows (v. 12.0K, SPSS Inc., Chicago, IL, USA) with a significance level of  $p < 0.05$ . The differences among the values of  $\text{SSI}^2$ ,  $\text{FSI}^2$ , SC, SBP, and ASTM were analyzed via one-way analysis of variance (ANOVA). The differences were considered to be statistically significant when  $p < 0.05$ . Post hoc tests were performed using the Bonferroni test. Pearson's correlation coefficient was used to assess the relationship between TE changes and the contrast values of EPSS and EPSC.

### 3. Results

#### 3.1. Phantom Study

Figure 4 shows the changes in gadoteridol SIs according to the TE controls in the phantom study.

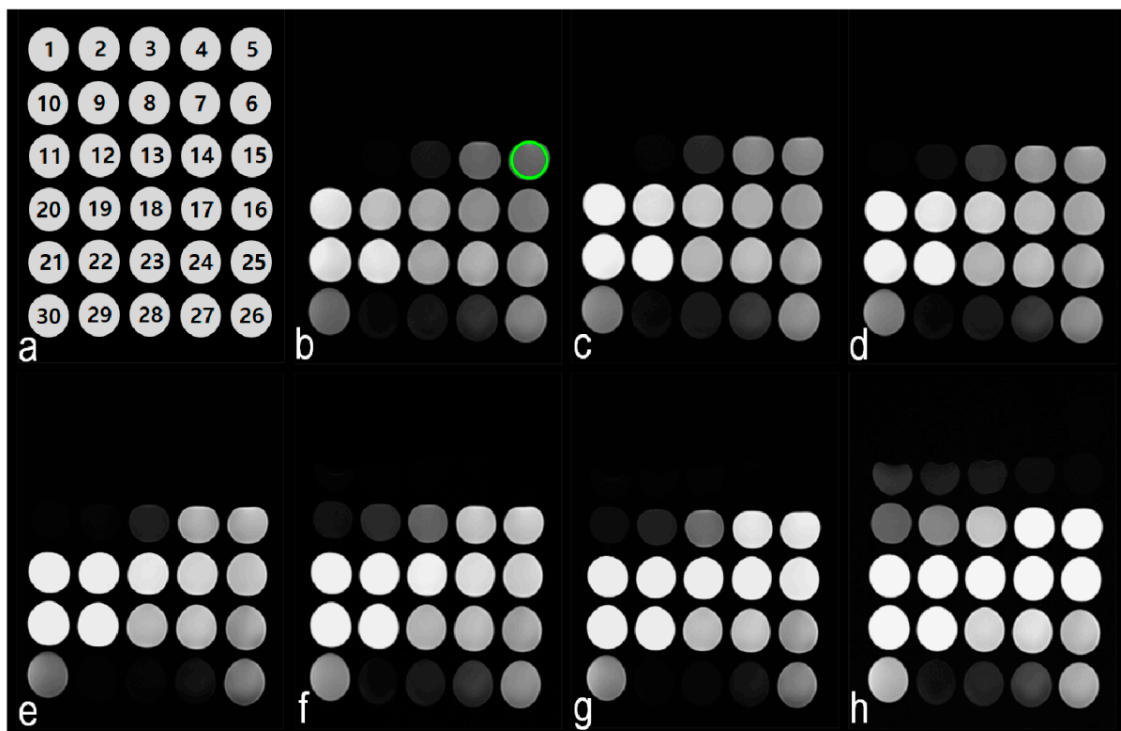


**Figure 4.** Phantom study images. (a) MR phantom container numbers; (b) changes in GBCA SI for a 25 msec TE; (c) changes in GBCA SI for a 22 msec TE; (d) changes in GBCA SI for a 19 msec TE; (e) changes in GBCA SI for a 16 msec TE; (f) changes in GBCA SI for a 13 msec TE; (g) changes in GBCA SI for a 10 msec TE; (h) changes in GBCA SI for a 7 msec TE. MR, magnetic resonance; GBCA, gadolinium-based contrast agent; SI, signal intensity; TE, echo time.

### 3.2. Changes in GBCA SI

Figure 5 shows a graphical representation of the change in GBCA SIs in the MR phantom with varying TEs. Table 3 shows the results for SSI<sup>1</sup>, FSI<sup>1</sup>, CPFS, RSP, MPSI, MPP, EPMS, AST, and EP. As the TE decreased from 25 to 7 msec, SSI<sup>1</sup> changed from 100 to 112 a.u., and FSI<sup>1</sup> increased from 840 to 1236 a.u. Consequently, with decreasing TE, CPFS also increased from 740.0 to 1003.6%. RSP was found to be between 30 and 90 mmol, while MPSI increased from 1771 to 2425 a.u., and MPP changed from 2 to 4 mmol, while EPMS changed from 1671.0 to 2065.2%. AST increased from 600.8 to 996.6 a.u. with decreasing TEs. Table 3 shows the changes in EP mmol for each concentration with varying TE.

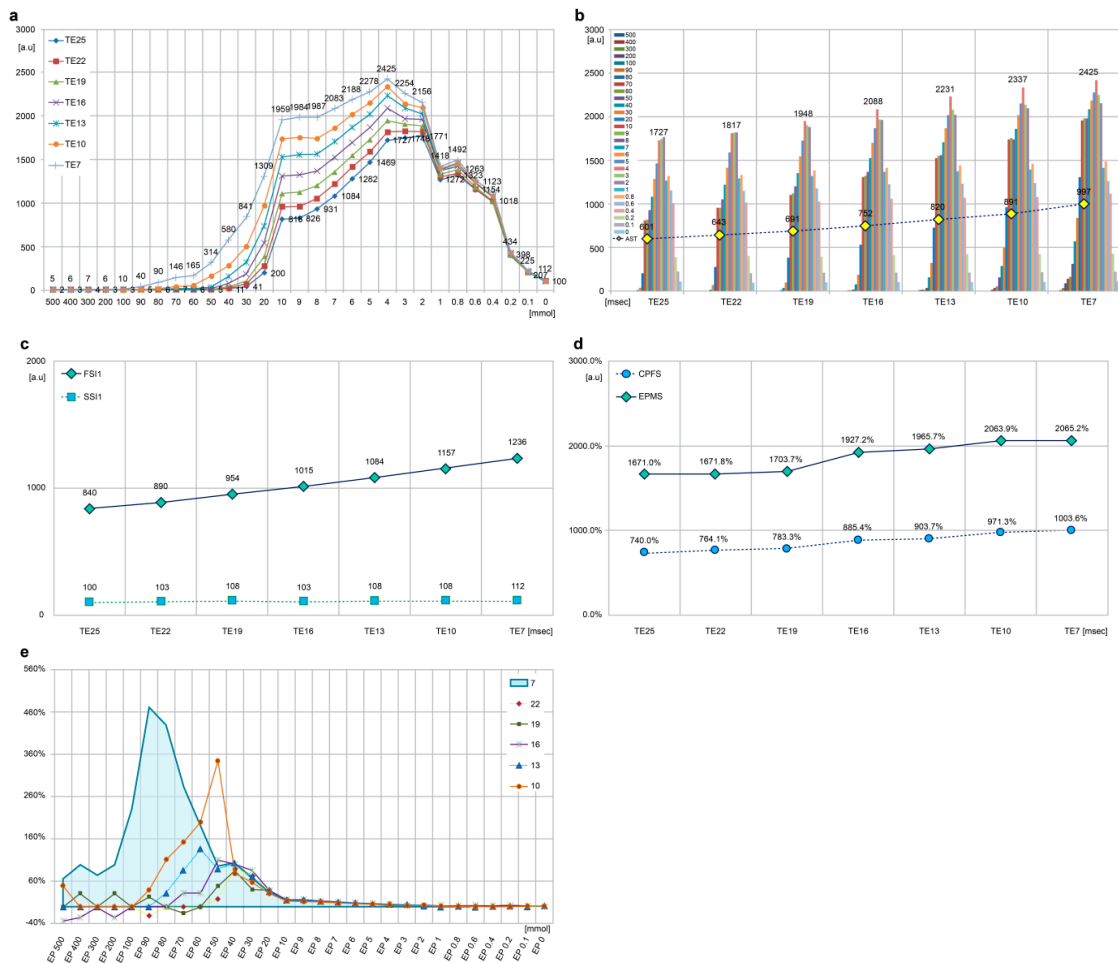


**Figure 5.** Graphs of signal changes according to various conditions. (a) Signal changes at each TE by concentration; (b) signal changes at each concentration and AST by TE; (c) saline and fat signal changes at each TE; (d) CPFS and EPMS signal changes at each TE; (e) EP changes at each concentration. TE, echo time; AST, average of SI for each mol per TE; CPFS, contrast percentage of fat to saline; EPMS, enhancement percentage of MPSI to saline; MPSI, max peak signal intensity; EP, enhancement percentage; SSI1, saline signal intensity of phantom study; FSI1, fat signal intensity of phantom study.

**Table 3.** Quantitative data for the different evaluation criteria in the phantom study.

TE	msec	25	22	19	16	13	10	7
SSI <sup>1</sup>	[a.u.]	100	103	108	103	108	108	112
FSI <sup>1</sup>	[a.u.]	840	890	954	1015	1084	1157	1236
CPFS	%	740.0	764.1	783.3	885.4	903.7	971.3	1003.6
RSP	mmol	30	30	30	40	40	60	90
	%	6	6	6	8	8	12	18
MPSI	[a.u.]	1771	1825	1948	2088	2231	2337	2425
MPP	mmol	2	3	4	4	4	4	4
	%	0.4	0.6	0.8	0.8	0.8	0.8	0.8
EPMS	%	1671.0	1671.8	1703.7	1927.2	1965.7	2063.9	2065.2
AST	[a.u.]	600.8	642.5	690.9	751.9	820.2	891.3	996.6
Factor (mmol, %)		22	19	16	13	10	7	
EP 500		50.5	0.0	−33.3	0.0	50.0	66.7	
EP 400		0.0	33.3	−25.0	0.0	0.0	100.0	
EP 300		0.0	0.0	0.0	0.0	0.0	75.0	
EP 200		0.0	33.3	−25.0	0.0	0.0	100.0	
EP 100		0.0	0.0	0.0	0.0	0.0	233.3	
EP 90		−20.0	25.0	0.0	0.0	40.0	471.4	
EP 80		0.0	0.0	0.0	33.3	112.5	429.4	
EP 70		0.0	−14.3	33.3	87.5	153.3	284.2	
EP 60		0.0	0.0	33.3	137.5	200.0	189.5	
EP 50		20.0	50.0	111.1	89.5	344.4	96.3	
EP 40		90.9	85.7	100	103.8	78.6	104.2	
EP 30		73.2	40.8	86.0	71.5	58.3	66.5	
EP 20		40.0	38.2	39.3	36.4	32.0	34.9	
EP 10		17.8	15.7	18.0	16.3	14.0	12.7	
EP 9		16.6	16.8	17.6	17.5	12.9	13.0	
EP 8		13.5	13.9	13.7	14.1	11.6	14.0	
EP 7		12.6	11.4	12.1	11.9	9.3	11.7	
EP 6		10.7	9.2	9.6	10.1	7.9	8.4	
EP 5		8.4	8.7	8.0	8.1	6.5	5.9	
EP 4		5.2	7.2	7.2	6.8	4.8	3.8	
EP 3		4.4	4.5	3.3	6.0	2.5	5.3	
EP 2		2.9	3.6	4.1	3.2	3.5	2.9	
EP 1		2.2	2.2	3.5	0.4	1.4	1.3	
EP 0.8		1.4	3.1	2.8	1.8	1.1	1.9	
EP 0.6		0.3	2.2	3.7	0.6	0.9	1.4	
EP 0.4		0.4	0.4	3.2	1.8	0.4	3.8	
EP 0.2		3.0	−1.7	4.5	1.4	0.9	0.7	
EP 0.1		0.0	1.9	2.4	0.0	1.4	2.7	
EP 0		1.0	2.0	0.0	2.9	1.9	3.7	

TE, echo time; SSI<sup>1</sup>, saline signal intensity of the phantom study; FSI<sup>1</sup>, fat signal intensity of the phantom study; CPFS, contrast percentage of fat to saline; RSP, response start point; MPSI, max peak signal intensity; MPP, max peak point; EPMS, enhancement percentage of MPSI to saline; AST, average of SI on each mol as TE; EP, enhancement percentage.

### 3.3. Clinical Study

Figure 6 shows images from the clinical study. The SI of the brain parenchyma and clinical phantom were compared with varying TEs. To this end, the SI was measured in the clinical phantom and in selected ROIs within the CSF and the brain parenchyma, as shown in Figure 6. According to the statistical analyses, there was not a significant difference between SSI<sup>2</sup> and SC. Table 4 shows the SSI<sup>2</sup>, FSI<sup>2</sup>, SC, SBP, ASTM, EPSS, SEPSS, EPSC, and AEPSC for different TEs. As TE was decreased from 25 to 7 msec, SSI<sup>2</sup> and SC did not show a significant change, while FSI<sup>2</sup>, SBP, and ASTM showed increasing patterns from 804 to 1106, 278 to 389, and 378 to 845 a.u., respectively. EPSS and EPSC were calculated as shown in Table 4; the respective averages for these values, AEPSS and AEPSC, both

increased with shorter TE, from 47.0 to 140.3% and from 224.3 to 647.8%, respectively. The correlation coefficients were calculated to determine the associations between TE change and the contrast values for EPSS and EPSC, which presented significant negative correlations for most values.

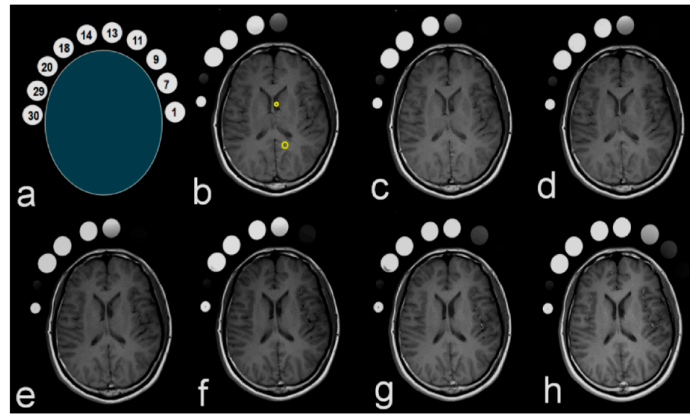


**Figure 6.** Images of the clinical study. (a) container numbers for the clinical phantom; (b) changes in SI for a 25 msec TE; (c) changes in SI for a 22 msec TE; (d) changes in SI for a 19 msec TE; (e) changes in SI for a 16 msec TE; (f) changes in SI for a 13 msec TE; (g) changes in SI for a 10 msec TE; (h) changes in SI for a 7 msec TE. SI, signal intensity; TE, echo time.

**Table 4.** Quantitative data for the different evaluation criteria in the clinical study.

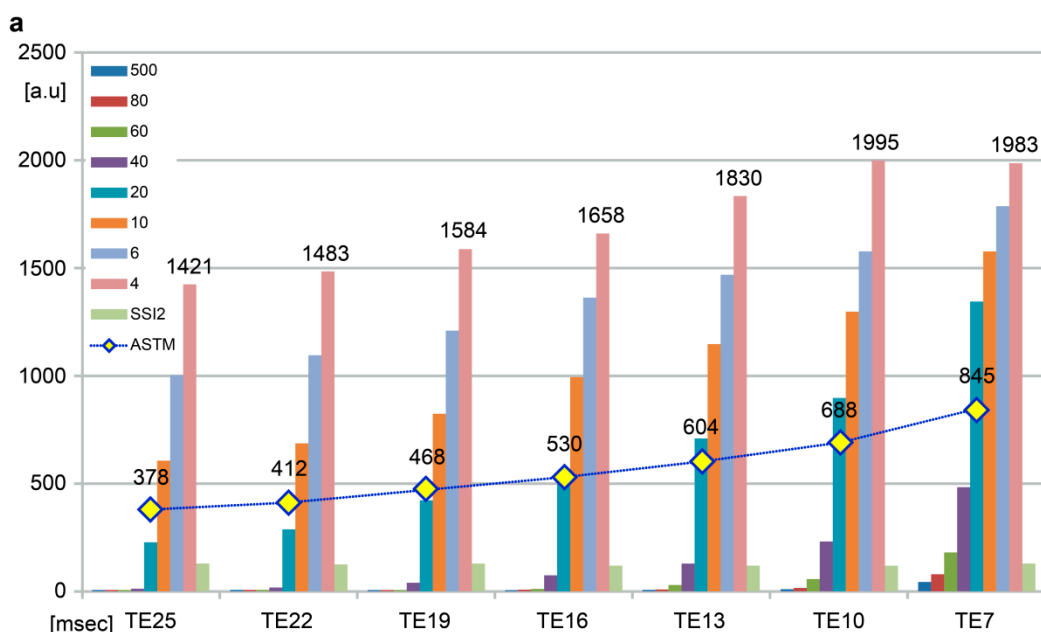
Factor	Unit	Clinical Study									
TE	msec	25	22	19	16	13	10	7	F	p-value	
SSI <sup>2</sup> <sup>b d e</sup>		129	126	129	120	120	121	128			
FSI <sup>2</sup> <sup>a c d e</sup>		804	819	887	961	911	982	1106			
SC <sup>b d e</sup>	[a.u.]	126	125	125	128	124	130	125	100.18	0.000	
SBP <sup>a b c e</sup>		278	310	321	342	357	376	389			
ASTM <sup>a b c d</sup>		378	412	468	530	604	688	845			
TE	msec	25	22	19	16	13	10	7	Correlation coefficients	p-value	
EPSS[500]		-98.9	-98.7	-99.1	-99.1	-98.9	-98.7	-89.5	-0.621	0.134	
EPSS[80]		-98.2	-98.7	-98.8	-99.1	-98.3	-95.7	-79.9	-0.679	0.094	
EPSS[60]		-99.3	-99.0	-98.8	-97.4	-93.0	-84.8	-53.2	-0.794	0.033 *	
EPSS[40]		-96.8	-94.2	-88.2	-79.5	-63.6	-38.8	24.4	-0.889	0.007 *	
EPSS[20]	%	-19.1	-7.1	30.8	61.4	98.6	138.0	246.5	-0.961	0.001*	
EPSS[10]		116.5	121.3	156.7	190.9	220.4	244.9	305.4	-0.984	0.000 *	
EPSS[6]		260.4	252.6	276.6	297.7	311.8	319.4	358.9	-0.964	0.000*	
EPSS[4]		411.2	378.4	393.5	384.8	412.6	430.6	409.8	-0.505	0.218	
AEPSS		47.0	44.3	59.1	70.0	86.2	101.9	140.3	-0.951	0.001 *	
EPSC[500]		-97.6	-96.8	-97.6	-97.7	-96.8	-96.2	-67.2	-0.635	0.125	
EPSC[80]		-96.0	-96.8	-96.8	-97.7	-95.2	-87.7	-37.6	-0.685	0.090	
EPSC[60]		-98.4	-97.6	-96.8	-93.0	-79.8	-56.2	45.6	-0.784	0.037 *	
EPSC[40]		-92.9	-86.6	-69.6	-45.3	4.8	76.9	287.2	-0.876	0.010 *	
EPSC[20]	%	78.6	130.4	236.0	331.3	471.8	588.5	978.4	-0.953	0.001 *	
EPSC[10]		377.8	448.8	559.2	677.3	822.6	897.7	1161.6	-0.989	0.000 *	
EPSC[6]		695.2	774.4	867.2	962.5	1085.5	1113.1	1328.0	-0.987	0.000 *	
EPSC[4]		1027.8	1086.4	1167.2	1195.3	1375.8	1434.6	1486.4	-0.984	0.000 *	
AEPSC		224.3	257.9	308.6	354.1	436.1	483.8	647.8	-0.969	0.000 *	

<sup>a</sup>  $p < 0.05$  versus SSF<sup>2</sup>, <sup>b</sup>  $p < 0.05$  versus FSF<sup>2</sup>, <sup>c</sup>  $p < 0.05$  versus SC, <sup>d</sup>  $p < 0.05$  versus SBP, <sup>e</sup>  $p < 0.05$  versus ASTM, \*  $p < 0.05$ . TE, echo time; SSI<sup>1</sup>, saline signal intensity of the phantom study; FSI<sup>1</sup>, fat signal intensity of the phantom study; SC, SI of the intraventricular cerebrospinal fluid; SBP, SI of brain parenchyma; ASTM, average of SI per TE for each molar concentration. EPSS, the enhancement percentage of SI for each mol by SBP; AEPSS, average EPSS; EPSC, enhancement percentage of SI for each mol by SC; AEPSC, average EPSC.

#### 4. Discussion

Previous studies have already addressed the characteristics of normal body tissues or lesions in T1 images by external parameters, but there is a lack of data regarding the SI changes of GBCA due to TE. Furthermore, GBCAs have been used clinically for the purpose of T1 enhancement without detailed information regarding the relationship between the parameters and response of gadolinium. However, the experiments in this study indicated that the extent of signal enhancement in T1 imaging is affected by TE. First, as shown in Figure 5c, the phantom study examined the effect of TE on signal enhancement between water and fat. Specifically, as the TE was decreased, there was almost no change in SSI<sup>1</sup>, but there was a gradual increase in FSI<sup>1</sup>. This is because the energy transfer efficiency in fat, which is a carbon-based macromolecule, was better than that of saline in a free water state. The CPFS graph in Figure 5d shows how changing TE affected the contrast between free water and fat. In terms of contrast enhancement, as shown in Figure 5b, AST increased with decreasing TE. Likewise, as shown in Table 4 and Figure 5a, RSP was earlier for shorter TE, meaning that the visible contrast enhancement response formed more rapidly. Decreasing TE was also associated with increased MPSI and earlier formation of the MPP. Consequently, EPMS also increased with decreasing TE, as shown in Figure 5d. In order to compare the improvement in contrast enhancement between different concentrations, we quantified the improvement and expressed this as EP; as shown in Figure 5e, decreasing TE was associated with a shift in the peak of the graph toward higher concentrations. In particular, signal enhancement was greatest at TE 7 msec, which means that the GBCA response was faster at TE 7 msec, resulting in greater signal enhancement. In other words, the phantom study demonstrated that diagnostically useful contrast enhancement can be achieved by decreasing TE.

We also conducted a clinical study for direct comparisons with brain images, and obtained the following results. First, as seen in Figure 6, the GBCA signal enhancement at low concentrations was visibly increased in the clinical phantom as TE was decreased. Indeed, the ASTM graph in Figure 7a demonstrates increasing SI with decreasing TE. In order to compare the free water SI of saline in the clinical phantom and CSF in the body, we produced the graph in Figure 7b. Little difference was observed between the values at all TEs, with both measures varying in the range 120–130 a.u. In other words, the SI in free water was similar in the clinical phantom to that in the body. The SI in the brain parenchyma was higher than in free water, as shown by the SBP in Figure 7b, and FSI<sup>2</sup> was even higher than SBP. Here, SBP and FSI<sup>2</sup>, with a constant molecular weight, showed an increase in signal with decreasing TE, whereas there was little change in the CSF signal.



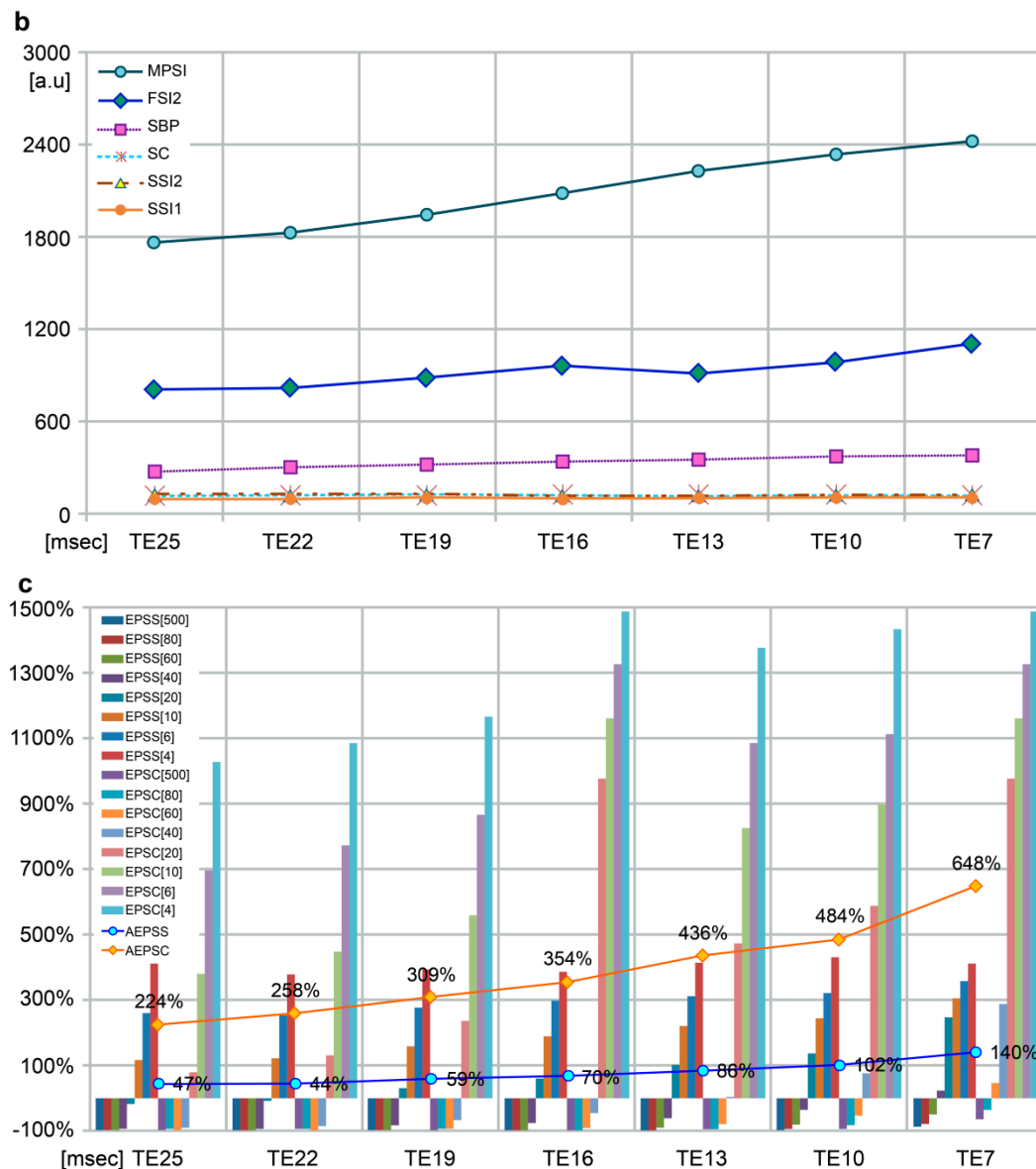


**Figure 7.** Graphs of SI changes in the clinical study. (a) changes in SI at different concentrations and ASTM by TE; (b) changes in SSI<sup>1</sup>, SSI<sup>2</sup>, FSI<sup>2</sup>, SBP, SC, and MPSI, by TE; (c) changes in EPSS, AEPSS, EPSC, and AEPSC by TE. SI, signal intensity; ASTM, average of SI per TE for each molar concentration; TE, echo time; SSI<sup>1</sup>, saline signal intensity of the phantom study, SSI<sup>2</sup>, saline signal intensity in the clinical phantom; FSI<sup>2</sup>, fat signal intensity of the second phantom, SBP, SI of brain parenchyma; SC, SI of the intraventricular cerebrospinal fluid; MPSI, max peak signal intensity; EPSS, the enhancement percentage of SI for each mol by SBP; AEPSS, average EPSS; EPSC, enhancement percentage of SI for each mol by SC; AEPSC, average EPSC.

Usually, when GBCA is delivered into the body, it mixes with the blood, resulting in a decrease in GBCA concentration over time. Based on this principle, each container in the clinical phantom can be considered to represent a mass or cancer. We obtained the contrasts between each phantom container and the brain images in Figure 6 as percentages, and compared the effect of TE on contrast enhancement in each container with that of the brain parenchyma, in order to quantify this contrast. For this purpose, we calculated EPSS and EPSC, as well as their corresponding averages, AEPSS and AEPSC, and have displayed these measures in both Table 4 and Figure 7c. Figure 7c shows a gradual increase in AEPSS and AEPSC with decreasing TE. Thus, if the phantom is considered to represent a tumor, given the

decreasing GBCA concentrations after delivery into the body, minimizing the TE provided an overall increase in tumor contrast enhancement compared to healthy tissue. Based on the results of both the phantom and clinical studies, we found that both a faster and higher signal enhancement in CE-T1 by using a shorter TE. Moreover, a short TE in T1 imaging is useful for increasing contrast with brain parenchyma structures in the T1 effect examinations. In summary, in CE-T1 imaging, using a short TE facilitates differentiation of basic structures, provides faster contrast enhancement, and increases the extent of contrast enhancement. However, our study had a limitation that needs to be acknowledged. Although there are two methods for T1 effect: spin echo (SE) and turbo spin echo (TSE), the present study examined only the effects of changes in the TE parameter on T1 imaging using conventional SE, which has been usually used for T1 effect in the clinical field [2,7,8]. Therefore, further research with TSE should be performed in order to set a lower TE than that achieved with SE. Despite this limitation, our study findings are clinically relevant as we re-evaluated whether the TE parameter is being set appropriately in current, routine CE-T1 imaging and further demonstrated that TE adjustment can provide better contrast enhancement for diagnostic purposes.

## 5. Conclusions

GBCA interactions with  $^1\text{H}$  spin in the body produces a contrast enhancement response according to MR physics control; our study demonstrated quantitatively that this response can be adjusted by changing the external MR parameters. Previous studies have only addressed the characteristics of normal body tissues or lesions in T1 images according to sequences, showing clinical comparison data according to GBCA concentration. However, the results of the present study suggest TE to be the optimal parameter for contrast enhancement of MRI T1 images clinically. The phantom and clinical studies both showed that as TE was decreased, MPSI increased, and RSP and MPP were formed earlier. Moreover, AEPSS and AEPSC were also improved. In conclusion, using the lowest possible TE for CE-T1 weighted MRI may provide a more useful diagnostic MR image.

**Author Contributions:** Conceptualization, H.K.J.; Methodology, H.K.J.; Software, H.K.J.; Validation, H.K.J.; Formal Analysis, H.K.J.; Investigation, H.K.J.; Resources and Statistics, K.H.L., S.H.K. and M.H.K.; Visualization, H.K.J.; Supervision, M.G.K. and H.C.K.

**Funding:** This research received no external funding.

**Conflicts of Interest:** The authors declare no conflict of interest.

## References

1. Hagberg, G.E.; Scheffler, K. Effect of  $r_1$  and  $r_2$  relaxivity of gadolinium-based contrast agents on the  $T_1$ -weighted MR signal at increasing magnetic field strengths. *Contrast Media Mol. Imaging* **2013**, *8*, 456–465. [[CrossRef](#)] [[PubMed](#)]
2. Seidl, Z.; Vymazal, J.; Mechl, M.; Goyal, M.; Herman, M.; Colosimo, C.; Pasowicz, M.; Yeung, R.; Paraniak-Gieszczyk, B.; Yemen, B.; et al. Does higher gadolinium concentration play a role in the morphologic assessment of brain tumors? Results of a multicenter intraindividual crossover comparison of gadobutrol versus gadobenate dimeglumine (the MERIT Study). *AJNR Am. J. Neuroradiol.* **2012**, *33*, 1050–1058. [[CrossRef](#)] [[PubMed](#)]
3. Bloembergen, N.; Purcell, E.M.; Pound, R.V. Relaxation effects in nuclear magnetic resonance absorption. *Phys. Rev.* **1948**, *73*, 679. [[CrossRef](#)]
4. Bloembergen, N. Proton relaxation times in paramagnetic solution. *J. Chem. Phys.* **1957**, *27*, 572. [[CrossRef](#)]
5. Just, M.; Thelen, M. Tissue characterization with  $t_1$ ,  $t_2$ , and proton density values: results in 160 patients with brain tumors. *Radiology* **1988**, *169*, 779–785. [[CrossRef](#)] [[PubMed](#)]
6. Maravilla, K.R.; Smith, M.P.; Vymazal, J.; Goyal, M.; Herman, M.; Baima, J.J.; Babbal, R.; Vaneckova, M.; Žižka, J.; Colosimo, C.; et al. Are there differences between macrocyclic gadolinium contrast agents for brain tumor imaging? Results of a multicenter intraindividual crossover comparison of gadobutrol with gadoteridol (the TRUTH study). *AJNR Am. J. Neuroradiol.* **2015**, *36*, 14–23. [[CrossRef](#)] [[PubMed](#)]

7. Maravilla, K.R.; San-Juan, D.; Kim, S.J.; Elizondo-Riojas, G.; Fink, J.R.; Escobar, W.; Bag, A.; Roberts, D.R.; Hao, J.; Pitrou, C.; et al. Comparison of gadoterate meglumine and gadobutrol in the MRI diagnosis of primary brain tumors: A double-blind randomized controlled intraindividual crossover study (the REMIND study). *AJNR Am. J. Neuroradiol.* **2017**, *38*, 1681–1688. [[CrossRef](#)] [[PubMed](#)]
8. Van Walderveen, M.A.A.; Barkhof, F.; Hommes, O.R.; Polman, C.H.; Tobi, H.; Frequin, S.T.; Valk, J. Correlating MRI and clinical disease activity in multiple sclerosis: relevance of hypointense lesions on short-TR/short-TE (T1-weighted) spin-echo images. *Neurology* **1995**, *45*, 1684–1690. [[CrossRef](#)] [[PubMed](#)]
9. Shen, W.C.; Cheng, T.Y.; Lee, S.K.; Ho, Y.J.; Lee, K.R. Disseminated tuberculomas in spinal cord and brain demonstrated by MRI with gadolinium-DTPA. *Neuroradiology* **1993**, *35*, 213–215. [[CrossRef](#)] [[PubMed](#)]
10. Owen, N.J.; Sohaib, S.A.; Peppercorn, P.D.; Monson, J.P.; Grossman, A.B.; Besser, G.M.; Reznek, R.H. MRI of pancreatic neuroendocrine tumours. *Br. J. Radiol.* **2001**, *74*, 968–973. [[CrossRef](#)] [[PubMed](#)]
11. Thomsen, H.S.; Morcos, S.K.; Almen, T.; Bellin, M.F.; Bertolotto, M.; Bongartz, G.; Clement, O.; Leander, P.; Heinz-Peer, G.; Reimer, P.; et al. Nephrogenic systemic fibrosis and gadolinium-based contrast media: updated ESUR Contrast Medium Safety Committee guidelines. *Eur. Radiol.* **2013**, *23*, 307–318. [[CrossRef](#)] [[PubMed](#)]



© 2018 by the authors. Licensee MDPI, Basel, Switzerland. This article is an open access article distributed under the terms and conditions of the Creative Commons Attribution (CC BY) license (<http://creativecommons.org/licenses/by/4.0/>).